

## GENERATIVE MODEL TO PREDICT THE DEFORMATION FIELD OF CFRP LAMINATES CONSIDERING GEOMETRIC AND PHYSICAL PARAMETERS IN WING ASSEMBLY

YUMING LIU\*<sup>1</sup>, YONG ZHAO<sup>2</sup>, QINGYUAN LIN<sup>3</sup>, WEI PAN<sup>4</sup>, YU REN<sup>5</sup> AND WENCAI YU<sup>6</sup>

<sup>1</sup> Shanghai Jiaotong University  
[Liu389658558@sjtu.edu.cn](mailto:Liu389658558@sjtu.edu.cn)

<sup>2</sup> Shanghai Jiaotong University  
[zhaoyong@sjtu.edu.cn](mailto:zhaoyong@sjtu.edu.cn)

<sup>3</sup> Shanghai Jiaotong University  
[qyuan\\_lin@163.com](mailto:qyuan_lin@163.com)

<sup>4</sup> Shanghai Jiaotong University  
[pwmogic666@sjtu.edu.cn](mailto:pwmogic666@sjtu.edu.cn)

<sup>5</sup> Shanghai Jiaotong University  
[xcution@sjtu.edu.cn](mailto:xcution@sjtu.edu.cn)

<sup>6</sup> Shanghai Jiaotong University  
[yu790876644@sjtu.edu.cn](mailto:yu790876644@sjtu.edu.cn)

**Key words:** Assembly analysis; Deformation prediction; Feature fusion; Deep learning; Generative model.

**Abstract:** Thin-walled structure of CFRP laminates is widely utilized in the assembly of aircraft wings. The deformation field generated during the assembly process can impact the assembly performance of the structure, thereby influencing the product quality and operational performance of the wings. The geometric deviations on the critical mating surfaces of the laminate and physical parameters are key factors influencing the deformation fields during the assembly process. Analyzing the mapping relationship between fusion assembly data and deformation field plays a crucial role for assessing the assembly results. The traditional analysis methods only consider the impact of simple directional deviations on assembly results and do not comprehensively account for the multi-source input. This paper proposes a multi-source assembly input -deformation analysis framework for CFRP bolted joints in aircraft wing assembly. Taking the parameters representing the geometric deviations and physical parameters as input and deformation field as output, a conditional generative model is employed to learn the influence pattern of the geometric deviations on the deformation field. The framework establishes a prediction model from the deviation field to the deformation field and introduces specific accuracy metrics. Corresponding simulations demonstrate that the proposed method can predict assembly deformation field more efficiently than traditional numerical methods. It

exhibits excellent performance on the accuracy metrics, enabling accurate and efficient field-to-field predictions. The predicted results can serve as a research framework for predicting other physical fields.

## 1 INTRODUCTION

Advanced composite materials, due to their high strength, high stiffness, high corrosion resistance, and designable mechanical properties, are extensively used in the structures of aircraft. However, the assessment and control of the assembly quality of composite structures largely rely on engineering experience and lack corresponding assembly design theories and methods. To balance the geometrics and performance in composite material structures used in mechanical products, it is necessary to explore the interaction laws between geometric quantities and the mechanical performance parameters during the assembly process[1].

Modeling variables during the assembly process is an essential component of high-performance assembly for composite materials, which can be categorized into geometric variables and performance variables. Researchers have developed various methods for geometric characterization, including modal decomposition models, deformation grid models, and skin model shape method. Huang et.al. [2] proposed the statistical models to generate geometric deviations, decomposing the deviation field into a limited number of fundamental deformation modes and employing modal decomposition to approximate the description of geometric deviations on surfaces. Franciosa et.al. [3] utilized a grid-based deformation method to describe geometric deviations in thin-walled parts. Anwer et al. introduced the concept of a skin model shape, which focuses on the detailed representation of surface deviations. Building on this, Scheich et.al. [4] developed an assembly deviation characterization and design framework based on the skin model shape. This framework integrates contact constraint optimization and the definition of differential surface, proposing a novel assembly simulation method grounded in skin model shape. This method aims to enhance the accuracy of simulating and predicting assembly processes, particularly in terms of managing and mitigating deviations, thereby improving overall assembly quality and performance. On the other hand, performance variables primarily include the physical performance parameters that influence the assembly outcome during the process. Modeling the flexible assembly process of composite material mechanical products requires a detailed understanding of these performance variables. Many scholars have focused on modeling the multi-station assembly process. Lin et.al. [5] combined the sub structuring method with statistical sampling techniques to reduce the calculation time, thereby accelerating the prediction efficiency of assembly deviations. Yi et.al. [6] further integrated error propagation theory and state space models to construct a framework for the error transmission and accumulation in multi-step assembly processes of complex products. The aforementioned methods have thoroughly investigated the impact of multiple factors on assembly outcomes. However, they rely on linear superposition approaches, which overlook the complex coupling relationships between geometric and performance variables. Consequently, they fail to achieve the construction of precise and efficient physical mapping models for composite material assembly under the influence of multiple input variables.

The deformation field resulting from the assembly process is a crucial factor in evaluating the physical field of the assembly system and is an important indicator of the geometric characteristics of the assembly outcome. Currently, many scholars have conducted in-depth

research on data-driven solutions for complex physical field prediction. the Generative Adversarial Networks (GANs), has demonstrated superior image reconstruction capabilities compared to other models [7]. By constructing a generator and a discriminator and training them simultaneously within a game-theoretic framework, the generator learns to "deceive" the discriminator's data distribution predictions, making it an effective tool for data inference. Yang et.al.[8] effectively applied this method to estimate stress and strain in complex composite material structures and proposed an end-to-end model construction method using cGAN to replace finite element calculations. Nie et.al. [9] also used the cGAN model to predict the impact of geometric shapes, loadings, and boundary conditions on the stress field. On the other hand, with the rise of Transformer models in the field of image processing, they have also been employed for generating physical fields. Jiang et. al. developed TransCFD [10] as a decoder to predict flow field results under aerodynamic shape parameters. Buehler et. al. [11] constructed FieldPerceiver based on an enhanced Transformer model, capable of effectively predicting physical field in microscale mechanics. However, current methods for predicting physical fields primarily focus on areas such as Computational Fluid Dynamics and microscale mechanics. There is a need to develop a framework suitable for predicting physical fields in composite material assembly. To address this, this paper establishes a framework for analyzing the deformation field of composite bolted joints under multiple sources of assembly factors. It proposes a data-driven deformation field prediction network called General characteristic-Multi modal-GAN (GC-MM-GAN), which achieves end-to-end prediction of composite bolted joints deformation fields for the whole assembly process. The effectiveness of the framework is validated through a case study of CFRP bolted joints used in wing assembly.

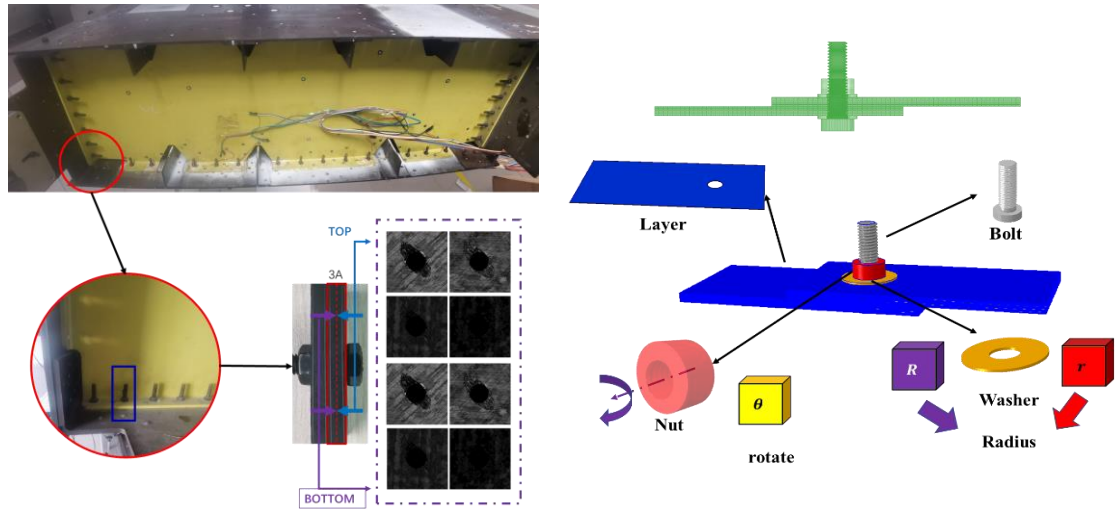
## 2 DIGITAL TWIN-ORIENTED PART SURFACE MODEL

During assembly, geometric errors may exist in the surface topography of parts. Geometric deviations at different scales can affect assembly results. Traditional deviation representations typically use tolerance interval constraint methods. The methods cannot consider the specific influence of morphology on assembly results, nor can they incorporate multi-scale geometric features into assembly analysis. Therefore, based on the skin model shape method, this paper constructs the geometric model of assembly components.

The modeling process for the component skin model shape mainly includes four steps: extraction of key mating surfaces from the nominal model, discretization of the surface, superposition of deviations at different scales, and reconstruction of solid elements containing physical features. The assembly model studied in this paper, as shown in the **Fig. 1(a)**, is a composite bolted joints used in wing assembly. The corresponding nominal model and parts are depicted in the **Fig. 1(b)**.

For the composite bolted joints discussed in this paper, the contact area of the laminates is the critical feature surface, which needs to be discretized and superimpose the deviations. For larger scale part surface deviations, methods like Discrete Cosine Transformation (DCT) or random field modeling are typically used. However, determining the weighting coefficients of various basis functions in the modal methods can be challenging, making it difficult to leverage historical statistical data effectively. Therefore, using random field representations that incorporate statistical parameters of the part surface is more suitable for addressing assembly process. This study utilizes non-Gaussian random fields to simulate surface topography based

on statistical data. This method is closer to reality than Gaussian random field simulation because different manufacturing processes can lead to non-Gaussian distributions of surface topography. Following the methodology outlined in **Ref.** [6], we combined the higher-order central moments of the laminate and washer surfaces heights to simulate non-Gaussian deviation distributions on a larger scale. The results of this simulation are shown in **Fig. 2**.



(a) CFRP bolted joints in the wing box (b) The CAD model of CFRP bolted joints  
**Fig. 1** Schematic of physical model and CAD model

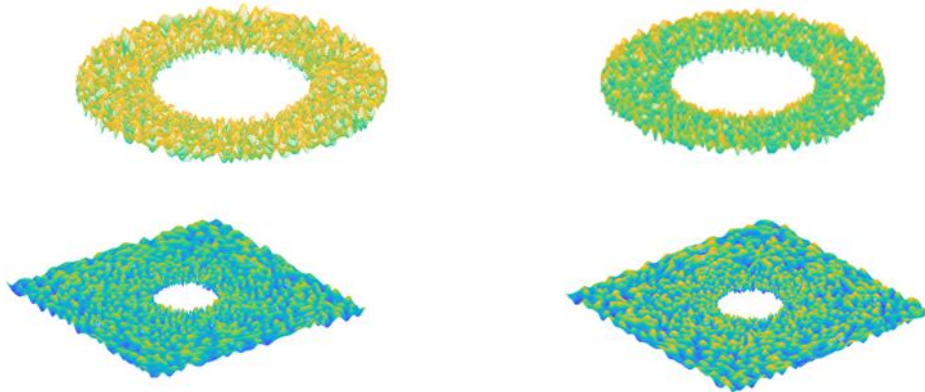


**Fig. 2** Simulation of surface morphology of washers and critical mating surfaces

For finer-scale morphology, simulating non-Gaussian random fields requires high-precision measurement equipment, and obtaining statistical parameters for a significant volume of parts is both difficult and expensive. Therefore, combining self-similar methods with fractal functions can infer the overall distribution from the topographical deviation structure of a part, further generating the fine-scale topography of the parts. This approach accounts for the elastic-plastic deformation of surface asperities and ensures that the overall model is deterministic, allowing for realistic simulation of part contact during assembly. This method proves to be practical and feasible for simulating the actual contact of components. In this study, we use the W-M function method to represent the surface morphology of the parts as the result of the superposition of different spectral cosine functions.

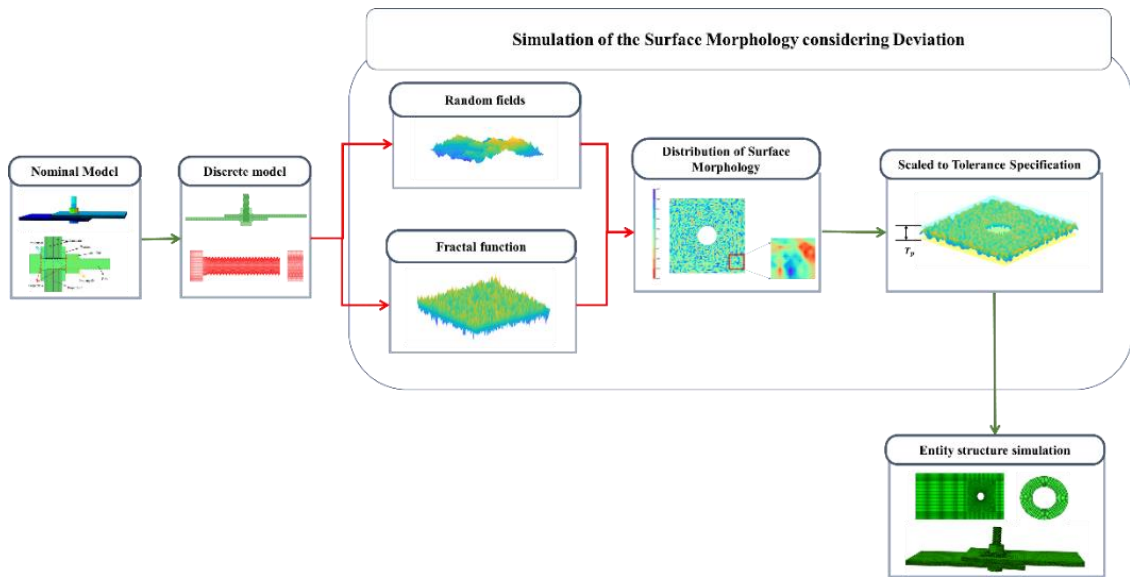


**Fig. 3** multi-scale part deviation modeling process

In summary, based on the generated results of multi-scale geometric deviations of key mating surfaces of assembly parts, the final skin model shape of the parts is obtained by superimposing these deviations within the given deviation interval constraints. After constructing the key morphology, the discrete point cloud is reconstructed into corresponding solid elements using the interpolation mesh method. It is worth noting that to ensure that the surface of the workpiece does not exhibit unrealistically large deviations, the overall error is often constrained by adding a tolerance band. Therefore, a more general multi-scale part surface morphology modeling process is summarized as shown in **Fig. 3**.

### 3 DATASET IMPLEMENTATION

As discussed before, the composite bolted joint structure for wing assembly consists of the composite laminate, the bolt, nuts, and washers' assemblies. To simulate the realistic tightening process of the composite bolted joint structure, a detailed threaded mesh model is established, as illustrated in **Fig. 4(a)**. Characterize the intra-laminar damage behaviors of CFRP using the continuum damage model (CDM). The determination of damage occurrence relies on the application of the 3D Hashin damage criteria. The progressive damage behaviors are characterized by modifying the stiffness matrix of the material as shown in **Fig. 4(b)**.

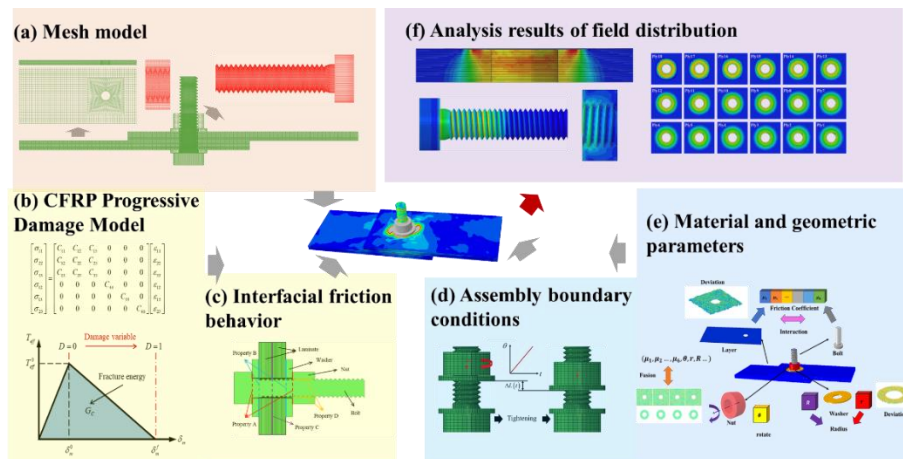


**Fig. 4** The process and principle of the dataset preparation

During the progressive damage analysis of the composite laminates, intra-laminar damage and inter-laminar damage are performed simultaneously. Then, we characterize the inter-laminar damage behaviors by using the cohesive contact method (CCM). As shown in **Fig. 4** (b), a bilinear traction-separation law is used to characterize the cohesive contact for the delamination processing.

The quadratic stress failure criterion is employed for the estimation of damage initiation, whereas the BK failure criterion is applied to forecast the propagation of delamination [12]. As shown in **Fig. 4** (c), a multitude of diverse contact pairs can be found in composite bolted joints. For the modeling of normal interactions, the default hard contact model, which prevents penetration of slave nodes into master surfaces, is employed. The classic Coulomb friction model is employed to represent the tangential behavior in all contact pairs between the constituent parts.

A dynamic explicit time step is introduced to simulate the authentic tightening process of the composite bolted joint, with control over the boundary conditions at the nut as shown in **Fig. 4**(d). The geometric data, material properties, and boundary conditions are further synthesized for finite element simulation, taking into account the variables as shown in **Fig. 6**(e). Extracting the normal compressive deformation fields on various laminates during the assembly process, as shown in **Fig. 4**(f), provides input for subsequent analysis.

Based on the aforementioned model and simulation methods, this study conducted Latin Hypercube sampling under various geometric and material parameters. The selection range of parameters and partition details of grids for the simulations are provided in **Table 1**.

After obtaining the displacement distribution data values, they were mapped to displacement contour plots through interpolation. The displacement results from FEM were interpolated to generate the contour plots of  $256 \times 256$  resolutions using bilinear interpolation. The images of the key feature surface of the washers and laminates are shown in **Fig. 5**(a), which serve as the input data. The deformation field cloud map under this morphology is prepared as shown in **Fig. 5**(b). Along with corresponding non-image data, the paired data is constructed for this study.

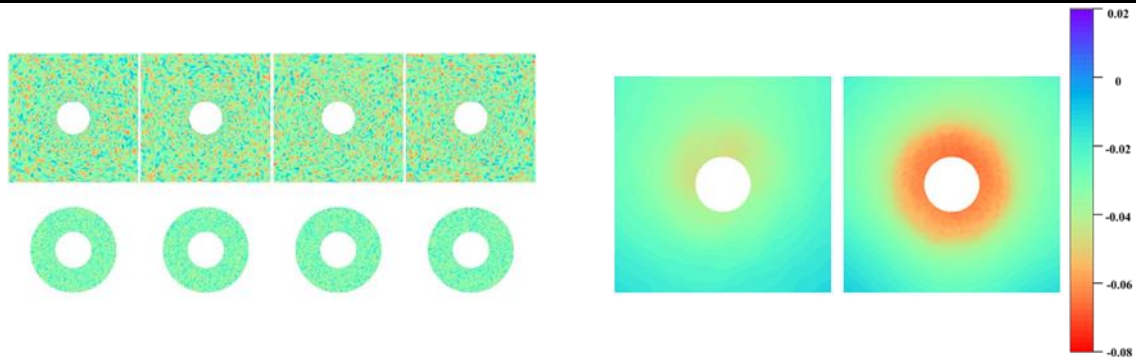
This study utilized 200 pairs of deformation cloud maps in the target region as the training and testing dataset. The preparation of the data was performed using the Siyuan-1 cluster

Random splitting and cross-validation methods were employed for the training and testing sets to eliminate biases.

**Table 1**

The parameter selection range and grid details for simulations

Meanings	Signal	Minimum	Maximum
Friction coefficient of bolt end face	$\mu_b$	0.1	0.5
Friction coefficient between washer and composite laminated plate	$\mu_{bc}$	0.1	0.5
Friction coefficient between composite laminates	$\mu_c$	0.1	0.5
Friction coefficient between nut and composite laminated plate	$\mu_{nc}$	0.1	0.5
Friction coefficient of nut end face	$\mu_n$	0.1	0.5
Thread friction coefficient	$\mu_t$	0.1	0.5
Bore radius of washer	$r_{in}$	3.0mm	3.5mm
Outer circle radius of washer	$r_{out}$	6.0mm	10.0mm
Thickness of washer	$t$	0.5mm	2.0mm
Nut tightening angle	$\theta$	0.16rad	1.36rad
Number of grids around holes	$N_{CC}$	64	96
Deviation of key feature surface	$T_p$	0mm	0.15mm



(a) The sample of parts' morphology

(b) The sample of deformation fields

**Fig. 5** Image preparation and sample results

#### 4 GC-MM-GAN MODEL ARCHITECTURE

The prediction framework in this study is based on a combination of a Vision Transformer (ViT) auxiliary network and a conditional Generative Adversarial Network (cGAN). The overall network architecture is illustrated in **Fig. 6**. The function of the ViT auxiliary network is to integrate image data and non-image information. What's more the sequence information could be embedded, such as assembly order, into a conditional latent space as learnable parameters. The cGAN module then uses the high-dimensional feature vectors output by the ViT auxiliary network as guiding conditions to generate the assembly result data field [13]. Ultimately, the GC-MM-GAN could output the deformation field prediction results similar to numerical analysis results under various inputs.

The VIT auxiliary network primarily includes a Transformer encoder module and a feature fusion module to achieve the integration of geometric and performance features. The Transformer block is used for feature extraction from image data. The image data represent the key mating area of the composite laminates. Additionally, the assembly sequence and position of different laminates during the assembly process affect the final results of the performance analysis. Non-image data are then integrated with the Transformer-encoded image data in the subsequent Mapping Network layer. The fusion method of the Mapping Network is shown in **Fig. 7(a)** where it stacks linear and convolutional layers to elevate the dimensionality of non-image data. This high-dimensional concatenation with the encoded image data forms conditional constraints in the latent space to guide the subsequent generation of field data.

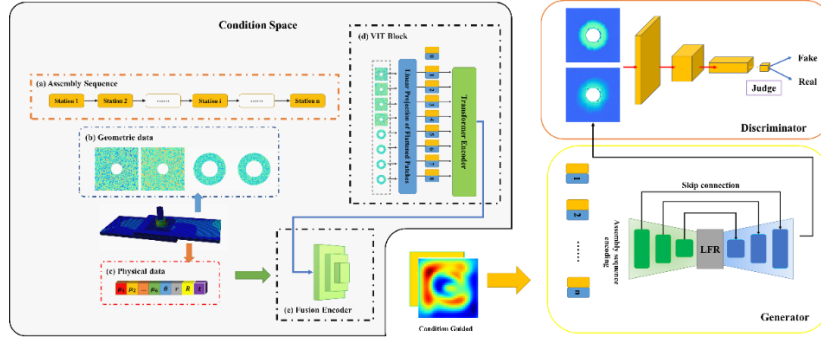


**Fig. 6** The architecture of GC-MM-GAN

For the generator, the U-Net structure is employed, as shown in **Fig. 7(b)**. The architecture primarily includes down-sampling encoding modules, up-sampling encoding modules, and skip connections. Down-sampling and up-sampling use convolution and transpose convolution operations, while skip connections enhance the network's ability to capture detailed field features, allowing for a more precise grasp of both global and local characteristics. Additionally, the down-sampling and up-sampling modules incorporate spectral normalization, which helps mitigate the training uncertainties introduced by the U-Net structure. This approach alleviates the artifacts generated during GAN training, achieving a good balance between enhancing local details and suppressing artifacts.

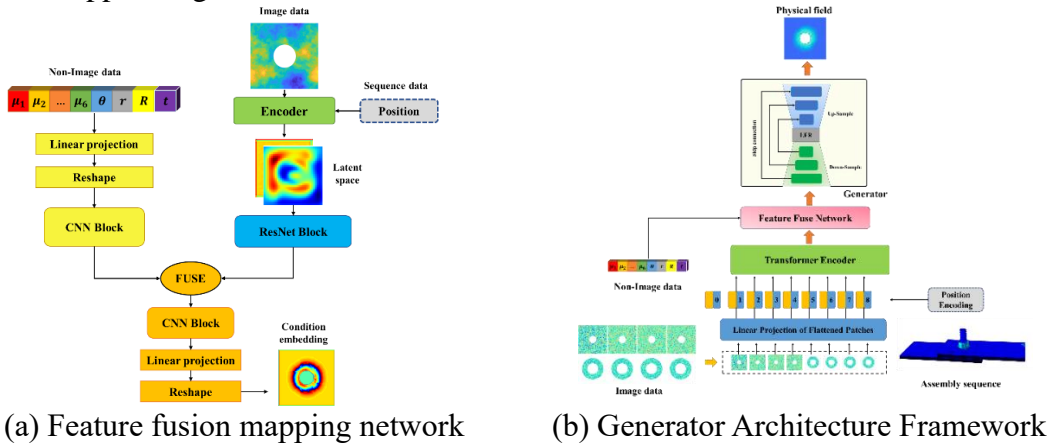


**Fig. 7** Description of the key component of the generator

The discriminator network employs the PatchGAN architecture, designed as a fully convolutional network as shown in **Fig. 8**. The input consists of deformation field images from assembly results, including real sample images generated by finite element simulation and



"fake" images generated by the generator. This discrimination method considers the local interrelationships within the physical field, representing the covariance and other statistical characteristics through pixel associations. By utilizing the network to recognize these complex couplings, the discriminator supervises the generator's learning direction, ensuring it learns the intricate rules of solving physical differential equations via finite element methods. The specific architecture consists of an input layer followed by a series of down-sampling modules. Each down-sampling module comprises 2D convolution, leaky ReLU, and instance normalization layers, which continuously extract key information from the images to ultimately perform authenticity verification.

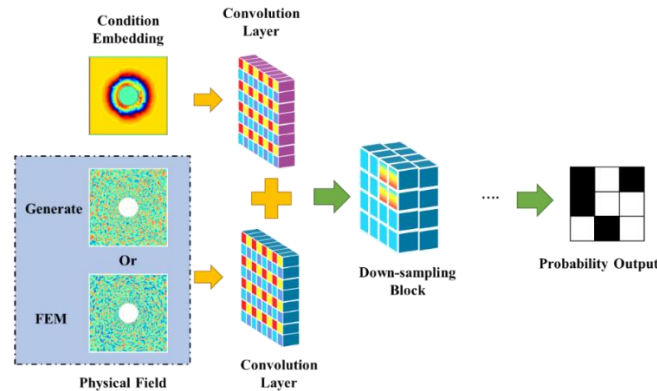


**Fig. 8** The structure of the discriminator

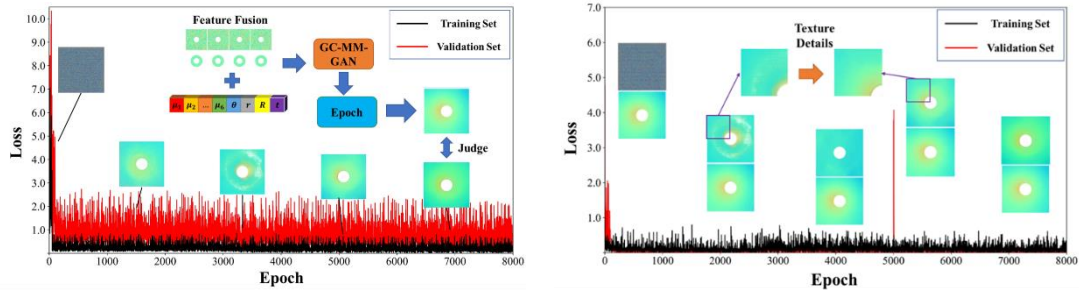
## 5 COMPUTATION RESULTS AND DISCUSSIONS

The training and testing errors for the generator and discriminator of GC-MM-GAN are shown in **Fig. 9(a)(b)**. The losses for both groups gradually decrease, and they converge after 400 epochs. Additionally, the deformation predictions at different stages are compared in the Figure. Initially, the generator can only produce simple shape features, with the deformation distribution still chaotic and disordered. After 5000 epochs, the generation quality improves significantly, though artifacts and local distribution differences remain in the image details. Through the adversarial training between the discriminator and generator, the generated details are progressively refined, resulting in cloud images that closely approximate the FEM results.

After training, the generator is utilized as a function approximator for the deformation field results fused with geometric deviations and physical parameters. It takes different geometric deviations and physical parameters as inputs and predicts the deformation field results for key areas, which are then compared with the results from FEM. The difference maps between the two are plotted. It can be observed that the predicted deformation cloud images are indistinguishable from the results of FEM to the naked eye. They effectively capture the overall trends of deformation distribution and some details around the holes. On the difference maps as shown in **Fig. 9(c)**, areas with significant prediction errors generally correspond to regions of deformation of abrupt changes, but they can still simulate and diagnose significant deformation anomalies. Following the evaluation metrics proposed in the previous section, a comparison is made among the CNN-MLP model, the model trained without discriminator, and GC-MM-GAN model. The comparison results of the corresponding metrics are shown in **Fig.**

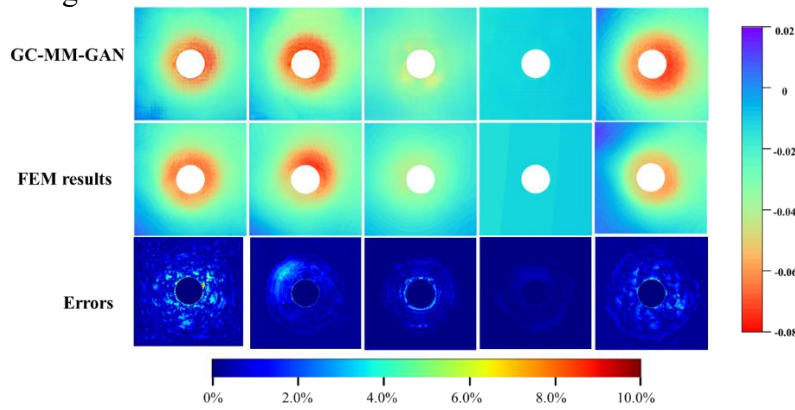
9(d)(e), with specific numerical values detailed in **Table 2**. It can be observed that our method not only achieves superior image quality in terms of similarity but also exhibits closer proximity at the data level.

Regarding the improvement in computational efficiency, a comparison is made between FEM and the trained GC-MM-GAN for a single case, as shown in **Table 3**. It can be seen that the speed of deformation prediction with the converged network is very fast. We can apply the GC-MM-GAN to further engineering deformation prediction and analysis, thereby saving a considerable amount of computational costs.

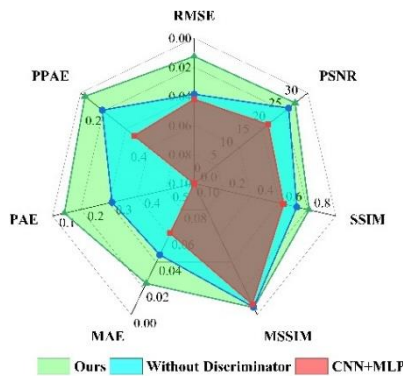


(a) The loss function variation of generator

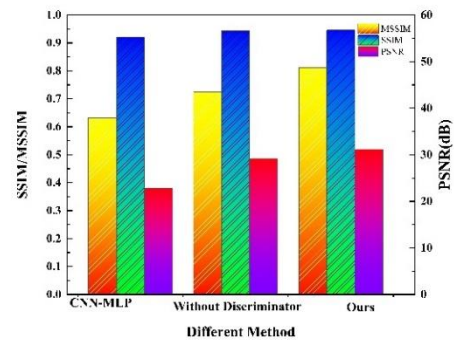
(b) The loss function variation of discriminator



(c) Comparison and difference figures of the deformation maps by GC-MM-GAN prediction and FEM calculations



(d) Performance radar plots of prediction results using different methods



(e) Comparison of image performance indicators of different methods

**Fig. 9** Network training and comparative verification of results

**Table 2**

Performance comparison of results from different methods

	SSIM	MSSIM	PSNR (dB)	RMSE	MAE	PAE	PPAE
CNN-MLP	0.632	0.9214	22.812	0.0421	0.0621	0.52	0.236
Without Discriminator	0.725	0.9435	29.125	0.0385	0.0456	0.21	0.095
<b>Ours</b>	<b>0.812</b>	<b>0.9458</b>	<b>31.125</b>	<b>0.0125</b>	<b>0.0238</b>	<b>0.042</b>	<b>0.0191</b>

**Table 3**

Comparison of the calculation time with FEM

Method	Time
Finite Element Method	25321.2s
Ours	4.1s

## 6 CONCLUSIONS

This study proposes a rapid deformation field prediction strategy for composite bolt structures based on deep learning. The fundamental idea is to utilize a cGAN-based network framework combined with a VIT auxiliary network to construct the deformation field prediction model GC-MM-GAN under multi-modal data input. This model takes geometric deviations and physical performance parameters during assembly as inputs, with the deformation field of key assembly areas as the target. Leveraging the results from progressive damage models and FEM, a database containing various interface states and deformation scenarios is established. Based on the current research, the following conclusions can be drawn:

(1) The prediction results of the GC-MM-GAN model on the test set under different conditions in the database were validated, and compared with several other models. According to various accuracy metrics proposed in this paper, GC-MM-GAN demonstrates stronger accuracy. Therefore, the good accuracy of the prediction model can be validated.

(2) Through the visualization of the features in the high-dimensional space layer during the training process, it is illustrated that the VIT auxiliary module plays a role in integrating geometric variables and physical variables, demonstrating the advantage of GC-MM-GAN in handling assembly multimodal data.

(3) The proposed GC-MM-GAN model needs to be further compared with other models and supplemented with comparative verification under different experiments to complete the model's transfer learning, which is an important task for future work.

## ACKNOWLEDGEMENT

This work was supported by the National Key Research and Development Program of China [Grant No. 2019YFA0709001], the National Key Research and Development Program of China [Grant No.2022YFF0605700] and the National Natural Science Foundation of China [Grant No. 51975349]. The computations in this paper were run on the Siyuan-1 cluster

supported by the Center for High Performance Computing at Shanghai Jiao Tong University. We are also thankful to Wu Guo from SJTU HPC for useful discussion.

## REFERENCES

- [1] Q. Liu, Y. Lin, Z. Zong, G. Sun, Q. Li, Lightweight design of carbon twill weave fabric composite body structure for electric vehicle, *Composite Structures* 97 (2013) 231–238.
- [2] W. Huang, Z. Kong, Simulation and integration of geometric and rigid body kinematics errors for assembly variation analysis, *Journal of Manufacturing Systems* 27 (2008) 36–44.
- [3] P. Franciosa, S. Gerbino, S. Patalano, Simulation of variational compliant assemblies with shape errors based on morphing mesh approach, *Int J Adv Manuf Technol* 53 (2011) 47–61. <https://doi.org/10.1007/s00170-010-2839-4>.
- [4] B. Schleich, N. Anwer, L. Mathieu, S. Wartzack, Skin Model Shapes: A new paradigm shift for geometric variations modelling in mechanical engineering, *Computer-Aided Design* 50 (2014) 1–15.
- [5] J. Lin, S. Jin, C. Zheng, Z. Li, Y. Liu, Compliant assembly variation analysis of aeronautical panels using unified substructures with consideration of identical parts, *Computer-Aided Design* 57 (2014) 29–40.
- [6] Y. Yi, X. Liu, T. Liu, Z. Ni, A generic integrated approach of assembly tolerance analysis based on skin model shapes, *Proceedings of the Institution of Mechanical Engineers, Part B: Journal of Engineering Manufacture* 235 (2021) 689–704. <https://doi.org/10.1177/0954405420958862>.
- [7] I. Goodfellow, J. Pouget-Abadie, M. Mirza, B. Xu, D. Warde-Farley, S. Ozair, A. Courville, Y. Bengio, Generative adversarial networks, *Commun. ACM* 63 (2020) 139–144. <https://doi.org/10.1145/3422622>.
- [8] Z. Yang, C.-H. Yu, M.J. Buehler, Deep learning model to predict complex stress and strain fields in hierarchical composites, *Sci. Adv.* 7 (2021) eabd7416. <https://doi.org/10.1126/sciadv.abd7416>.
- [9] H. Jiang, Z. Nie, R. Yeo, A.B. Farimani, L.B. Kara, Stressgan: A generative deep learning model for two-dimensional stress distribution prediction, *Journal of Applied Mechanics* 88 (2021) 051005.
- [10] J. Jiang, G. Li, Y. Jiang, L. Zhang, X. Deng, TransCFD: A transformer-based decoder for flow field prediction, *Engineering Applications of Artificial Intelligence* 123 (2023) 106340. <https://doi.org/10.1016/j.engappai.2023.106340>.
- [11] M.J. Buehler, FieldPerceiver: Domain agnostic transformer model to predict multiscale physical fields and nonlinear material properties through neural ologs, *Materials Today* 57 (2022) 9–25.
- [12] Y. Liu, Q. Lin, W. Pan, W. Yu, Y. Ren, Y. Zhao, Sr-M-Gan: A Generative Model for High-Fidelity Stress Fields Prediction of the Composite Bolted Joints, Available at SSRN 4650285 (n.d.). [https://papers.ssrn.com/sol3/papers.cfm?abstract\\_id=4650285](https://papers.ssrn.com/sol3/papers.cfm?abstract_id=4650285) (accessed December 5, 2023).
- [13] Y. Jadhav, J. Berthel, C. Hu, R. Panat, J. Beuth, A. Barati Farimani, Stressd: 2d Stress Estimation Using Denoising Diffusion Model, Available at SSRN 4478596 (n.d.).